DEUTSCHES ELEKTRONEN-SYNCHROTRON DESY

DESY 88-085
June 1988

QCD EFFECTS IN HADRONIC FINAL STATES AT HERA

by

M. Bengtsson

Institut für Theoretische Physik, RWTH, Aachen

G. Ingelman, B. Naroska

Deutsches Elektronen-Synchrotron DESY, Hamburg

ISSN 0418-9833

NOTKESTRASSE 85 · 2 HAMBURG 52

To be sure that your preprints are promptly included in the
HIGH ENERGY PHYSICS INDEX ,
send them to the following address (if possible by air mail) :

DESY
Bibliothek
Notkestrasse 85
2 Hamburg 52
Germany

DESY 88-085
June 1988

ISSN 0418-9833

QCD Effects in Hadronic Final States at HERA[1]

M. Bengtsson[a], G. Ingelman[b], B. Naroska[b]

[a] Institut für Theoretische Physik, RWTH, D-5100 Aachen, FRG
[b] Deutsches Elektronen-Synchrotron DESY, Notkestrasse 85, D-2000 Hamburg 52, FRG

Abstract

QCD effects in the hadronic final state of deep inelastic events are investigated using models based on exact first order matrix elements and parton cascade evolution in the leading log approximation. Large effects are observed in inclusive $p_\perp$ distributions as well as in angular energy flows and energy correlation functions. Higher order contributions in the cascade approach show sizeable effects, making a first order model less realistic. The measurement of α_s or Λ_{QCD} is difficult within the theoretically less well-defined parton cascade, but may be achieved through jet ratios dominated by first order effects.

1 Introduction

The presence of QCD phenomena in the hadronic final state of deep inelastic scattering events has been observed in fixed target experiments. Viewed in the hadron system centre-of-mass (boson-proton rest frame) high-$p_\perp$ particle production, occurence of planar events and a two-jet structure in the forward (current jet) hemisphere have been observed [1,2]. These effects are not only qualitatively as expected from QCD, but also quantitative agreement with first order perturbative QCD has been demonstrated [1-4]. Other predicted phenomena, such as the angular energy flow asymmetry and azimuthal asymmetries, are not observable at the limited energy scale ($Q^2 \lesssim 100$ GeV^2, $W \lesssim 20$ GeV) of fixed target experiments due to large smearing effects arising in the non-perturbative hadronization process [4]. With the increased phase space available for parton radiation at HERA energies, $Q^2 \lesssim 4 \times 10^4$ GeV^2 and $W \lesssim 300$ GeV, these QCD effects should become observable and a larger fraction of *resolvable* multijet events is also expected to emerge.

The purpose of this study is to demonstrate QCD effects at HERA energies in several observables and examine their suitability for more quantitative tests, in particular a measurement of α_s or Λ_{QCD}. As will be clear from our results, these are two rather different issues since large QCD effects do not necessarily imply a good measurement of α_s or Λ. This is due to the well known problems of finding a model that is both theoretically well-defined and which describes the data accurately enough.

We first discuss the theory and models that are necessary for a meaningful comparison with data, section 2, and then investigate general observables, such as inclusive $p_\perp$ spectra, in section 3. The suggested angular energy flow and possible energy-energy correlations are considered in section 4. Ratios of jet multiplicites as a measure of α_s are investigated in section 5 and we end with a concluding discussion in section 6.

[1] Contribution to the DESY workshop on Physics at HERA, Hamburg, October 1987.

2 Theory and models

First order QCD involves the two processes in Fig. 1a and b: gluon radiation, $V+q \rightarrow q+g$, and boson-gluon fusion, $V+g \rightarrow q+\bar{q}$ (V denotes the exchanged γ, Z^0 or $W^{\pm}$ boson). The matrix elements [5] are five-fold differential in the normal deep inelastic variables x, Q^2 and three additional variables for the internal degrees of freedom of the emerging two-parton system, corresponding e.g. to the energy and angles of the final quark. A procedure for efficient Monte Carlo simulation of events according to these matrix elements is discussed in [6,7]. The soft and collinear divergences are avoided by requiring a minimum invariant mass of all parton pairs. Similar to e^+e^- annihilation this is formulated in terms of the scaled variable $y_{ij} = m_{ij}^2/W^2 > y_{min}$. y_{min} is choosen as small as possible to take also some softer radiation into account; in particular, it should be smaller than any experimental jet resolution so that no observable jet emission is lost.

The natural frame for these studies is the hadronic CM frame, i.e. the rest system of the interacting boson and proton which also define a suitable axis for longitudinal momenta with the forward direction along the boson momentum. The invariant mass, W, of this system is furthermore the primary scale for the QCD effects. Although Q^2 is used as scale in α_s, the x-dependence of the matrix elements make $W^2 = Q^2(1-x)/x$ the more relevant scale for transverse momentum effects, e.g. $< p_\perp^2 > \propto W^2$ (see first paper in [5]), which is also verified experimentally [1]. The matrix elements further predict the largest effects in the forward hemisphere and a clear forward-backward asymmetry in agreement with the expectations has also been observed [1,2].

In going to the HERA energy domain these QCD effects are expected to become larger, in spite of a smaller α_s (due to the increased Q^2). This is mainly due to the increased phase space available for QCD radiation, which leads to more observable effects, e.g. multijet events can be accomodated. Thus, higher order QCD corrections will be important. We note that the available W values go up to $\sim$ 300 GeV, i.e. far above the PETRA energy region where α_s^2 and still higher order effects have been observed to be relevant [8]. The tree diagrams to order α_s^2 are being calculated for a large cutoff, y_{min}, corresponding to hard and well separated jets [9]. The full calculation, including virtual corrections, is much more complicated and will require a considerable effort. We note that the complete second order is needed in order to properly define the scale used as argument in α_s and a Λ parameter in a well-defined renormalization scheme. Nevertheless, the partial result will give useful jet cross-sections.

Based on experience from PETRA, where second order matrix elements have been important but found not to be adequate to describe multicluster events [8], it is likely that yet higher orders will be important also at HERA. At present, the only way to handle these is through a parton cascade or shower evolution in the leading log approximation as illustrated in Fig. 1c. Such a model can also describe the internal properties of high-$p_\perp$ jets in $p\bar{p}$ collisions reasonably well [10]. A model of this kind, which simulates dynamically both initial and final state parton radiation, has recently been developed for deep inelastic scattering [11]. Although the schemes developed for e^+e^- annihilation and $p\bar{p}$ collsions can essentially be taken over, there are important new problems, e.g. due to kinematics constraints from the lepton vertex [11].

The general problems and limitations of the parton shower approach are, of course, present also in this application. It is only a scheme within the leading log approximation and therefore expected to work better for soft emission than for hard. This implies that the widening and softening of jets [12] will be well described but not necessarily the absolute rate of multijet events. An artificial, and not gauge invariant, separation of initial and final state radiation is made which cannot take interferences between the two into account. A cutoff between this perturbative evolution and the following hadronization is needed, but its value is not specified and hence must be taken as a free parameter to be adjusted using real data and depending on the fragmentation model used. A scale for the maximum virtuality (off-shell mass-squared) of the quark initiating the shower (at the boson

vertex) is also needed. The naive choice would be Q^2, but as mentioned above W^2 is the more relevant effective scale in first order matrix elements. In particular, since Q^2 is usually smaller than W^2 a tail to large $p_\perp$ present in the matrix elements would be lost if a Q^2 scale were used. Thus, W^2 seems to be the better scale choice and will be used in the following, but we note that the two scales (and hence also the results) are essentially the same unless x is small.

For matrix elements and parton showers alike, the parton state can be hadronized using the Lund string model [13,14] to obtain a complete Monte Carlo event generation model [6,11] which we use in the following investigations. The advantages and disadvantages of the matrix element (ME) and parton shower (PS) aproaches are discussed in [11]. For present energy fixed target experiments, both kinds of models can be tuned to describe the hadronic final state quite well [15]. At HERA energies, however, the parton shower approach is expected to provide a better description of the event complexity induced by higher order effects and will therefore be of larger practical use in spite of its theoretical shortcomings. In particular, the Λ parameter cannot be specified in a well-defined renormalization scheme. It would be preferable to merge the two schemes such that the exact matrix elements are used to correct the shower algorithm to give the proper rate of hard emission. This has been achieved to order α_s in e^+e^- [16], but is a much harder problem to solve for deep inelastic scattering [17] and a working model of this kind has not been available for this study.

3 Inclusive $p_\perp$ effects

For the following Monte Carlo simulation results we usually restrict the kinematics to the deep inelastic region, requiring both Q^2 and $W^2 > 10^3$ GeV^2. This also avoids the problematic low-x region mentioned above. Neutral current event samples corresponding to an integrated luminosity between 60 and 100 pb^{-1} are typically generated to illustrate the statistical precision obtainable in less than a year of HERA running. The two models, first order matrix elements (ME) and parton showers (PS), are compared for different observables and Λ varied to examine the sensitivity to this parameter.

The inclusive $p_\perp^2$-distribution of charged particles in the hadronic CM frame is shown in Fig. 2a. In comparison to the naive quark-parton model (QPM) a dramatic effect from QCD is seen. The strong energy dependence of the large-$p_\perp$ tail is seen by comparing with the fixed target result in Fig. 2b. There is a clear difference between forward and backward particles, which is increasing with energy and is accentuated when plotting $< p_\perp^2 > (x_F)$ as in Fig. 3. (The forward hemisphere, $x_F > 0$, is in the boson direction, or equivalently the current jet direction.) This first order matrix element prediction is not spoiled by the higher order emissions in the parton shower. Backward parton emission corresponds here to initial state gluon radiation, which is found to be both more central and suppressed relative to final state radiation as a result of phase space differences and a structure function related suppression of initial radiation [11]. Although the distribution in $p_\perp^2$ clearly demonstrates the occurence of hard QCD emission, it is not so sensitive to the higher order effects or variations of Λ. It is too inclusive an observable to be used as a measure of Λ.

4 Energy flows and correlations

The angular energy flow is defined by the energy-weighted cross-section, as a function of the parton/hadron polar angle with respect to the current axis in the hadronic CM frame. It has been suggested as an interesting observable, which reveals properties of the perturbative QCD matrix elements, see [4] and references therein. In first order QCD, radiated gluons tend to be along the scattered quark direction, thus producing a forward-backward asymmetry in the energy flow. For fixed target

energies, however, it has been shown that this effect is almost completely washed out by the transverse energy flow produced by fragmentation and resonance decays in the dominating 2-jetlike events (quark + diquark jets) [4]. On the other hand, the unequal fragmentation properties of the forward quark and backward diquark lead to a large asymmetry in the energy flow at fixed target energies. At HERA, these non-perturbative effects are expected to be less important, so that the measurable hadron energy flow should reveal the underlying parton level result from perturbative QCD. Monte Carlo studies show that this is indeed the case [15]; although the 2-jet events still give a sizeable hadron energy flow at large angles that reduce the observable effect, it is found to be smaller than that from QCD effects. The expected asymmetry should, therefore, be seen directly in the angular energy flow at HERA, Fig. 4a. Defining the asymmetry

$$A(\theta) = \frac{E(\theta) - E(\pi - \theta)}{E(\theta) + E(\pi - \theta)}, \quad 0 < \theta < \frac{\pi}{2}, \tag{1}$$

where $E(\theta)$ is the energy at polar angle θ, the effect is more clearly seen, Fig. 4b. Since the simple QPM model gives essentially no asymmetry (see [15]) this provides a clear qualitative test of QCD. Quantitative measurements, however, suffer from the same problems to be discussed in connection with energy flows below.

The energy-energy correlation (EEC) [18] has been a useful probe of QCD effects and the internal structure of jets [19] in e^+e^- annihilation. It is defined as:

$$\Sigma(\theta) = \frac{1}{N} \sum_{events} \sum_{i,j} \frac{E_i E_j}{s} \delta(\theta_{i,j} - \theta) \tag{2}$$

where $\theta_{i,j}$ is the angle between particles i and j. The asymmetry of the correlation (EECA) is particularly useful since fragmentation effects cancel to a large extent making, e.g., an α_s measurement less model dependent. One might therefore expect that these observables should be useful also in deep inelastic scattering, where the same analysis could be defined in the hadronic CM frame. This is however not the case for the following reasons.

In ep collisions the target jet is essentially lost in the beam pipe and consequently the cancellation effects in 2-jet events are not present, which makes the asymmetry less useful. Nevertheless, it is interesting to consider these observables as if the whole event were measurable. The EEC distribution receives contributions from hard QCD processes, with large event-by-event fluctuations, as well as from softer gluon emission and hadronization with smaller fluctuations due to a smaller momentum scale and larger multiplicities involved. The latter tend to cancel in the asymmetry, which should therefore be dominated by the hard emission. In leptoproduction, the total invariant mass is not available for hard QCD emission and, relative to e^+e^- annihilation, the soft processes have therefore a larger influence. This results in a very small asymmetry at large angles, which is not significantly sensitive to variations of Λ, and a large asymmetry peak at small angles due to the different fragmentation properties of the current (quark) jet and the target remnant (diquark) jet. Thus, even in this idealized case, the EECA is not as useful as in e^+e^- annihilation. In order to quantify the effect of lost acceptance due to the beam pipe, particles within 50 mrad from the beam axis were excluded from the Monte Carlo analysis. Since the asymmetry of the energy-energy correlation does not make much sense unless the starting point is a two-jet system the EEC distribution itself was used. At the parton level a difference of $\sim 30\%$ was found when changing Λ between 0.1 and 0.4 GeV. Unfortunately, this difference is completely washed out at the level of observable hadrons.

Although the hadronic CM frame is convenient for theoretical studies, there are experimental problems since the boost from the lab frame requires the knowledge of the event kinematics as well as particle masses. Studies in the lab frame are, therefore, important and the following method, suggested in [15], provides an alternative energy-energy correlation analysis that seems to give better

results than the one from e^+e^-. For each event, denote by η_i, ϕ_i, $E_{\perp i}$ the pseudorapidity, azimuthal angle and transverse energy of particle i (or calorimeter cell i) as measured in the HERA lab frame. Using the distance measure $\omega_{ij}^2 = (\eta_i - \eta_j)^2 + (\phi_i - \phi_j)^2$ in the $\eta - \phi$ space and with $p_\perp^2 = Q^2(1-y)$ of the scattered lepton as suitable normalization, the transverse energy-energy correlation at distance ω can be defined as

$$\Omega(\omega) = \frac{1}{N_{event}} \sum_{events} \sum_{i \neq j} \frac{E_{\perp i} E_{\perp j}}{Q^2(1-y)} \delta(\omega - \omega_{ij}). \tag{3}$$

The autocorrelation $i = j$ at the origin is not included and the δ function is smeared by the histogram bin width. The above problems with the target remnant jet are absent since the use of transverse energies (w.r.t. the beams) effectively suppresses the target remnant and instead enhances the current jet and QCD radiation effects related to it. The response of this function to details in the ME and PS models as well as fragmentation effects is studied in [15]. Here, only the final result is given, Fig. 5, to show the increasing broadness of the distribution as more QCD effects are added by going from the QPM model to first order ME and then to the PS model. The Monte Carlo data points in the PS case are for an event sample corresponding to an integrated luminosity of 60 pb^{-1} and demonstrate the very good precision with which this distribution can be measured. Comparing the two curves for different Λ one could infer a large sensitivity giving a quantitative QCD measurement. It should be realized, however, that the Λ parameter used in the PS case is not defined in a proper renormalization scheme and cannot give the same fundamental information as using exact matrix elements including the complete next-to-leading order corrections. The ME model, on the other hand, results in lower values at large ω, due to the lack of higher orders, and will probably be far below the real data. Nevertheless, one can use this observable to see first that the PS model works better, thereby demonstrating higher order effects, and then exploit the precision for detailed tuning of such models; perhaps excluding some alternative ones. If the parton shower method could be put on a firmer theoretical base, e.g. by matching with exact matrix elements, the extracted value of Λ could also be of importance.

5 Jet multiplicities and jet ratios

The problem of jet reconstruction at HERA has been investigated in [20] and shown to present no major problem provided that a suitable jet finding algorithm is used. In particular, the reconstructed jets were demonstrated to have a meaningful relation to the underlying parton processes and be only slightly smeared by experimental detector effects. An example of a jet multiplicity distribution is given in Fig. 6. The jets are defined by a UA1-like algorithm, summing the transverse energy within a cone $\Delta R = \sqrt{\Delta\eta^2 + \Delta\phi^2} < 0.5$ in the pseudorapidity-azimuthal angle space and requiring $E_{\perp jet} > 5$ GeV. (This will effectively exclude the target remnant jet.) As can be seen, jet multiplicities are quite accurately measured and are therefore of potential use for a measurement of α_s or Λ using ratios between the rates of different number of jets.

Multijet events can only be obtained in the parton shower model, where higher order corrections are included, and Fig. 6 shows a clear sensitivity to Λ. Due to the theoretical shortcomings of the model, as discussed above, this cannot be exploited for a measurement of the fundamental QCD parameter. We note, however, that the one- and two-jet rates are very similar in the ME and PS models and are therefore only mildly influenced by higher order corrections. This influence depends furthermore on the jet definition algorithm and can hence be minimized. The strategy for the following analysis is therefore to use a suitable jet reconstruction algorithm, tuned so as to suppress higher order multijet events. Given the agreement between the two models, one can use the theoretically better defined ME model to investigate the ratio of 2-jet events to 1-jet events as a measure of α_s. Note, that the target remnant jet is not counted here and these two event classes therefore naively correspond to the first order QCD processes and the pure QPM model, respectively.

The above mentioned jet finding algorithm, which is only applicable in the lab frame, is not suitable for this purpose. Firstly, the transverse momenta in the lab frame are not dominantly given by QCD effects but rather by the event kinematics; $p_\perp^2 = Q^2(1-y)$ for the current quark in the simple QPM model. With a current jet slightly above the minimum $E_{\perp jet}$, it is almost impossible to find a second jet simply because of momentum conservation. Secondly, small shifts can, via the steeply falling $E_{\perp jet}$ distribution, give rise to large fluctuations in the number of reconstructed jets. Such effects are observed in the transition from the parton to the hadron level, resulting in shifted 2-jet rates and a large discrepancy between these levels, which in turn introduces systematic uncertainties.

For our purposes it is thus better to perform the analysis in the hadronic CM frame, where more suitable jet algorithms similar to those used in e^+e^- physics can be applied. The proton remnant jet has still to be considered in order to avoid an extra jet sometimes being reconstructed and sometimes not depending on whether there happened to be particles from it outside the beam pipe or not [20]. In principle, the total momentum of the particles within the beam pipe can be reconstructed from momentum conservation (at least in neutral current events). Together with measured particles close to the beam pipe one may be able to reconstruct this jet with a good enough precision compared to the resolution of the jet algorithm, which is typically coarser than the beam pipe cone. In our simulation, therefore, we use the complete event for jet finding and then exclude the one corresponding to the target jet, i.e. reduce the jet multiplicity by one unit.

Different jet reconstruction algorithms, with different jet separation measures were considered. A scheme joining all particles (or calorimeter cells) as long as their invariant masses, $y_{ij} = m_{ij}^2/W^2$, are small enough would be possible [20]. It can, however, produce 'spurious' jets composed of low-momentum particles alone, which would upset the jet counting. This could be avoided by a slight redefinition of the algorithm, but we will instead use a similar scheme where this problem is avoided. In this algorithm [21] (LUCLUS in JETSET) particles are joined into clusters as long as their distance d_{ij} is smaller than a given resolution parameter d_{join}. The distance measure d_{ij} is related to the transverse momentum of one particle with respect to the other and hence d_{join} measures the maximum $p_\perp$ between particles in a jet. To choose the value of d_{join}, two criteria should be considered: (*i*) It should be large enough to include fluctuations from soft gluon emission and fragmentation effects within a jet. (*ii*) It should result in a statistically reasonable 2-jet sample. We will use two alternatives in the following; fixed $d_{join} = 5$ GeV which was found suitable for hadronic LEP events at the Z^0 resonance, and $d_{join} = 2.2 ln W - 5.5$ GeV in order to match the energy available for jet production. The latter is similar to applying the cut in a scaling variable, such as the y variable above, and rescales the jet resolution such that the increasing soft emission at higher energies is included in the jet definition.

In order to investigate the dependence on Q^2 and W^2, we collect the Monte Carlo data in the following bins:

$$Q^2 \;:\; 100-376,\ 376-1414,\ 1414-20000\ GeV^2 \tag{4}$$

$$W^2 \;:\; 1000-2714,\ 2714-7368,\ 7368-20000\ GeV^2 \tag{5}$$

which divide the considered range in $\log Q^2$ as 1/4, 1/4, 1/2 and similarly the $\log W^2$ region as 1/3, 1/3, 1/3. We note that the mean value of one variable within a bin does not vary much when the other variable is changed from bin to bin and there are, therefore, no strong effects of coupled kinematics. For the highest W^2 interval, higher order gluon emission becomes important and one has to choose d_{join} appropriately to include this extra emission. To estimate these higher order effects we have used the PS model and find a 3-jet/2-jet ratio of typically 10%. This gives some confidence that a reasonable jet reconstruction is made and that the result is dominated by 1- and 2-jet events described by the order α_s matrix elements.

Resulting 2-jet/1-jet ratios are given in Fig. 7, for jets reconstructed both from the partons and at the final hadron level, in each case for two values of the Λ-parameter. The statistical errors obtainable

with $\sim$ 100 pb^{-1} are either explicitly shown or within the size of the symbol itself. Clearly, the statistical precision will not be the limiting factor in this kind of study. In the lowest Q^2 bin, which has the largest statistics, the increase of the 2-jet/1-jet ratio with W for a fixed jet resolution is shown in Fig. 7a and the rather constant ratio obtained with the energy dependent jet resolution parameter in Fig. 7b. The former alternative corresponds to a given detector with a given jet resolution and illustrates the increased jet activity with increasing energy, whereas a scaling jet resolution is often better for theoretical analyses. A very good agreement between the parton jet ratios and the hadronic ones is achieved for large W values, but at low W where the jets are less well separated fragmentation effects are more important and induce clear differences.

The Q^2 dependence of the jet ratio is given in Fig. 7c, for large W using the fixed jet resolution, and shows an increase with Q^2. The nice correspondence between parton and hadron jets is to a large extent destroyed at larger Q^2 values. Therefore, we use the lower Q^2 region, which has also the best statistical precision, in combination with the highest W interval, where a better hadron-parton correspondence was seen, to examine the dependence on the Λ parameter in more detail. This is shown in Fig. 8, where the corresponding mean values of α_s are also indicated. It deserves to be noted that in this kinematical region, the current quark is at a large angle to the proton beam; for the mean Q^2 and W^2 values the angle is 58^0 using QPM kinematics. This indicates that the second jet is not very close to the beam pipe and should not interfere with the target jet or be affected by the beam pipe hole. Considering the very small statistic errors (approximately equal to the symbol sizes) together with the small systematic shift between the parton and hadron level results, a fairly good measurement of α_s should be possible. To the extent that the parton-hadron shift can be well understood, this need not enter fully in the effective error estimates. Thus, it is not trivial to estimate the error on α_s from Fig. 8 and we therefore refrain from giving a specific value. The measurement of α_s rather than Λ is here emphasized due to the absence of loop corrections that must be used to define the scale for α_s properly and then obtain a well-defined Λ parameter. The α_s measurement is thus the only possibility at present.

We note that even if a measurement of α_s with small errors cannot be obtained, there are still possibilities to give essentially model independent bounds on its value. A measured value of the 2-jet/1-jet ratio would give a lower bound on α_s, since this ratio is reduced in the parton to hadron transition, Figs. 7 to 9. The size of this reduction may vary in different hadronization models, but it seems very unlikely that an increase can occur in a realistic model. A stronger, but model dependent, bound can be obtained if the parton-to-hadron shift is unfolded based on a model that has been strongly constrained by the data. Upper bounds could be obtained by other observables, or processes, and thereby the value of α_s constrained to an allowed range.

Finally we address the problem of observing a running α_s. Using the highest W bin again, Fig. 9 shows the Q^2 variation of the 2-jet/1-jet ratio for the case of the standard running $\alpha_s(Q^2)$ and fixing it to the mean value in the lowest Q^2 bin, where the two cases consequently give the same results. A fixed α_s results in an essentially linear increase of the jet ratio with increasing Q^2, although the slope is different at the parton and hadron levels. A much lower rate at large Q^2 is observed for a running α_s and also a clearly different behaviour; with a rise followed by a flattening or turnover with increasing Q^2. This gives an indication that jet ratios can be used to observe a running α_s, but it must be emphasized that conclusive evidence relies on next-to-leading order corrections to fix the scale properly. Lacking this, the scale problem can be seen as a two-dimensional one involving both Q^2 and W^2: the proper scale can be some combination of the two. This can be investigated through the variation of the 2-jet/1-jet ratio in the Q^2, W^2 plane.

This jet ratio study contains some idealizations that may result in too favourable results. Both, charged and neutral particles have been used with their correct momenta in the jet reconstruction procedure. Using only charged particles, well measured in a tracking chamber, would significantly

reduce the considered jet ratio and thus enlarge the parton-hadron differences. Calorimeter measurements to include the neutral particles therefore seem necessary, but may on the other hand introduce larger measurement errors. (Lost neutrinos have no effects on these results.) Particle losses in the beam pipe have been briefly investigated and do not seem to be a problem, in accordance with the discussion above concerning the exclusion of the proton remnant jet.

6 Conclusions

The QCD effects in the hadronic final state are large at HERA energies and should be clearly seen in many observables, preferentially in the hadronic CM frame: large transverse momentum particles, a forward-backward asymmetry of $p_\perp$ effects and energy flows, the transverse energy-energy correlation as well as multijet events. To establish the occurence of QCD effects in agreement with expectations should therefore be rather straightforward. A precision test involving the actual measurement of α_s or Λ is, however, far more difficult as can be expected based on experience from e^+e^- physics at PETRA. HERA events will be less clean due to the proton remnant jet and more difficult to measure because of the forward-boosted event character in an ep collider. On the other hand, the invariant mass of the hadronic system extends to much higher values, which should make some effects clearer since the available phase space can accomodate more clearly separated jets in multijet events.

The analysis process will have to be a stepwise procedure. First different models are confronted with the data for a first tuning or total rejection, e.g. the order α_s model is expected to fail in many respects. Secondly, a fine tuning is necessary where the sensitivity to various parameters and other details are examined in detail. The scale choice problem in the parton shower model should e.g. be better constrained. Theoretical cross-checks between different schemes and models can also give a better understanding and theoretically more constrained models, e.g. a matching of the parton shower algorithm with exact low order matrix elements would be very useful. Given a successful result of these steps, an improved Monte Carlo model can be constructed for detailed comparisons with data. This could not only give an agreement with QCD expectations but also lead to the extraction of a value of α_s or Λ which is of theoretical relevance.

Examples of observables which are sensitive to variations of the Λ parameter were given, e.g. the transverse energy-energy correlation. These depend, however, on higher order effects that can presently only be described with parton shower models and thus not used to determine the fundamental Λ in QCD. The most promising way, therefore seems to be the use of jet ratios in a constrained analysis to have only one- and two-jet events that can be theoretically better controlled in terms of exact matrix elements.

The exploratory analysis presented here is certainly idealized with respect to experimental problems. Some theoretical problems are also pointed out, but not solved. Under these circumstances it is premature to specify an expected error in such an α_s measurement. Our main objective is rather to illuminate the problems and point out a promising method for such a measurement.

Figure Captions

Figure 1 Gluon radiation (a) and boson-gluon fusion (b) processes in first order QCD. (c) Initial and final state parton shower evolution.

Figure 2 Inclusive $p_\perp^2$ of charged particles in the hadronic CM frame. (a) Parton shower (PS) and matrix element (ME) models at HERA energy: $Q^2, W^2 > 10^3$ GeV^2. For clarity smoothed curves from the Monte Carlo simulations are shown, but in one case points with error bars corresponding to an integrated luminosity of 60 pb^{-1} is shown to indicate the statistical precision in a typical HERA experiment. (b) Fixed target energy with EMC data [2] and curves from the first order QCD model.

Figure 3 Average $p_\perp^2$ as a function of $x_F = 2p_z/W$ in the hadronic CM frame. Parton shower and matrix element model at HERA energy ($Q^2, W^2 > 10^3$) with curves and error bars as in Fig. 2a. Fixed target data (EMC) [2] are shown for comparison.

Figure 4 Angular energy flow (a) and its asymmetry (b) for HERA Monte Carlo events with $Q^2, W^2 > 10^3$ GeV^2. $z = E_h/W$ is the fractional hadron energy at angle θ, measured with respect to the current direction in the hadronic CM frame: otherwise notation as in Fig. 2a.

Figure 5 Transverse energy correlation function $\Omega(\omega)$, eq. (3), at HERA. Monte Carlo events with $Q^2, W^2 > 10^3$ GeV^2 based on the parton shower and matrix element models. The points with error bars, shown in one case, correspond to an integrated luminosity of 60 pb^{-1}.

Figure 6 Multiplicity distribution of reconstructed jets in the parton shower and matrix element models for HERA events. The statistical errors correspond to an integrated luminosity of 60 pb^{-1}.

Figure 7 Ratio of 2-jet events to 1-jet events (excluding the proton remnant jet) as a function of $\log W^2$ (a,b) and $\log Q^2$ (c). In (a) and (c) a fixed jet resolution, $d_{join} = 5$ GeV, has been used and in (b) one that scales with energy, $d_{join} = 2.23 ln W - 5.5$ giving mean values 2.85, 3.95 and 5.05 in the three W-bins. The selected Q^2, W^2 regions are specified. The results are for two values of the Λ parameter, 0.1 (squares) and 0.4 (circles) GeV, and for jet reconstruction at both the parton level (open symbols) and the final hadron level (full symbols). Error bars shown, or within symbol size, for data samples less than 100 pb^{-1}.

Figure 8 Dependence of the 2-jet/1-jet ratio on the Λ parameter value. Fixed jet resolution and notations as in Fig. 7. The corresponding mean values of α_s are also given.

Figure 9 Q^2 variation of the 2-jet/1-jet ratio for running α_s and fixing it to the value in the lowest Q^2 region. Notation as in Fig. 7.

References

[1] J.J. Aubert et al., EMC Collaboration, Phys. Lett. 95B (1980) 306; Phys. Lett. 100B (1981) 433; Phys. Lett. 130B (1983) 118
M. Arneodo et al., EMC Collaboration, Phys. Lett. 149B (1984) 415

[2] M. Arneodo et al., EMC Collaboration, Z. Phys. C36 (1987) 527

[3] B. Andersson, G. Gustafson, G. Ingelman, T. Sjöstrand, Z. Physik C9 (1981) 233

[4] G. Ingelman, B. Andersson, G. Gustafson, T. Sjöstrand, Nucl. Phys. B206 (1982) 239

[5] G. Altarelli, G. Martinelli, Phys. Lett. 76B (1978) 89
A. Méndez, Nucl. Phys. B145 (1978) 199
R. Peccei, R. Rückl, Nucl. Phys. B162 (1980) 125
Ch. Rumpf, G. Kramer, J. Willrodt, Z. Phys. C7 (1981) 337

[6] G. Ingelman, LEPTO version 5.2, DESY preprint in preparation

[7] G. Ingelman et al., 'Deep Inelastic Physics and Simulation', these proceedings

[8] JADE Collaboration, W. Bartel et al., Z. Phys. C33 (1986) 23
TASSO Collaboration, W. Braunschweig et al., Oxford Nuclear Physics 29/88 (1988), DESY 88-046

[9] J.G. Körner, E. Mirkes, G.A. Schuler, in preparation

[10] P. Ghez, G. Ingelman, Z. Phys. C33 (1987) 465

[11] M. Bengtsson, G. Ingelman, T. Sjöstrand, these proceedings
M. Bengtsson, T. Sjöstrand, Z. Phys. C37 (1988) 465
M. Bengtsson, G. Ingelman, T. Sjöstrand, Nucl. Phys. B301 (1988) 554

[12] For a recent review of jet physics see, e.g.,
G. Ingelman, DESY 87-145 and proc. XVth International Winter Meeting on Fundamental Physics 'Lepton nucleon interactions at high energies', Sevilla, Spain, 1987, Eds. F. Barreiro, J.L Sanchez-Gomez, World Scientific, p. 165

[13] B. Andersson, G. Gustafson, G. Ingelman, T. Sjöstrand, Phys. Rep. 97 (1983) 31

[14] T. Sjöstrand, Computer Phys. Comm. 39 (1986) 347
T. Sjöstrand, M. Bengtsson, Computer Phys. Comm. 43 (1987) 367

[15] M. Bengtsson, G. Ingelman, T. Sjöstrand, Nucl. Phys. B301 (1988) 554

[16] M. Bengtsson, T. Sjöstrand, Phys. Lett. 185B (1987) 435 and Nucl. Phys. B289 (1987) 810

[17] M. Bengtsson, Aachen preprint PITHA 88/11

[18] C. Basham, L. Brown, S. Ellis, S. Love, Phys. Rev. Lett. 41 (1978) 1585

[19] JADE Collaboration, W. Bartel et al., Z. Physik C25 (1984) 231

[20] P.N. Burrows, G. Ingelman, E. Ros, these proceedings

[21] T. Sjöstrand, Computer Phys. Comm. 28 (1983) 229

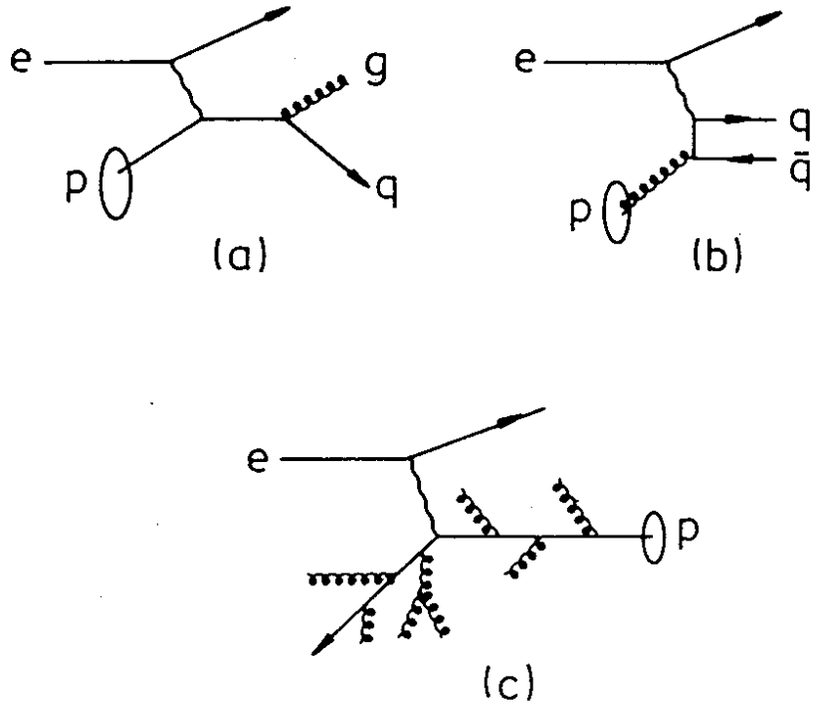

Fig. 1

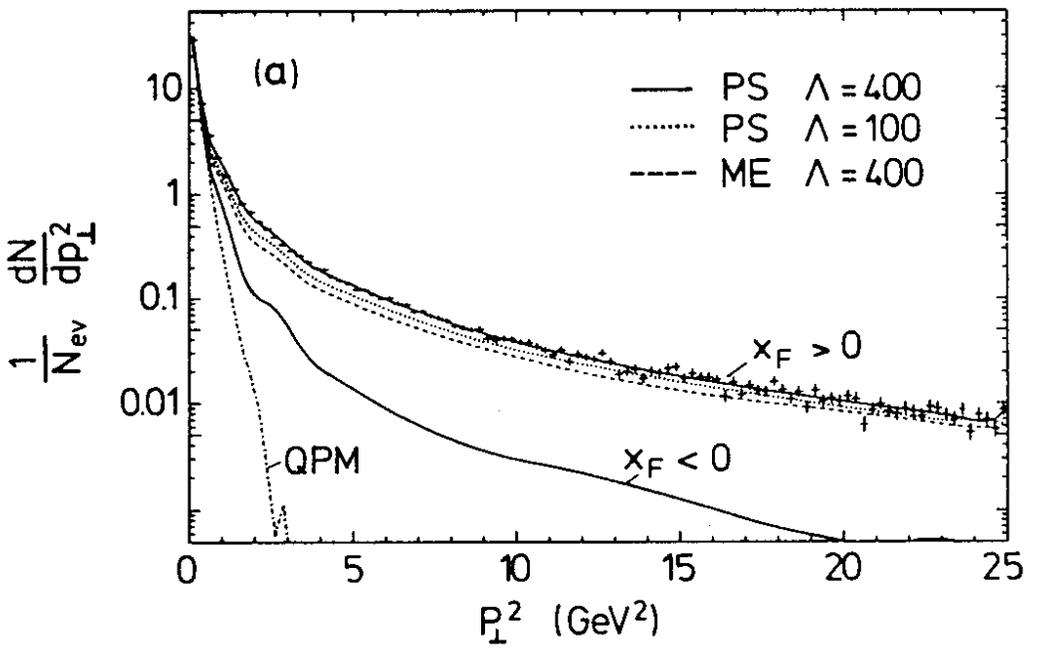
(a)
PS Λ = 400
PS Λ = 100
ME Λ = 400
$x_F > 0$
$x_F < 0$
QPM
$\frac{1}{N_{ev}} \frac{dN}{dp_\perp^2}$
$P_\perp^2$ (GeV^2)

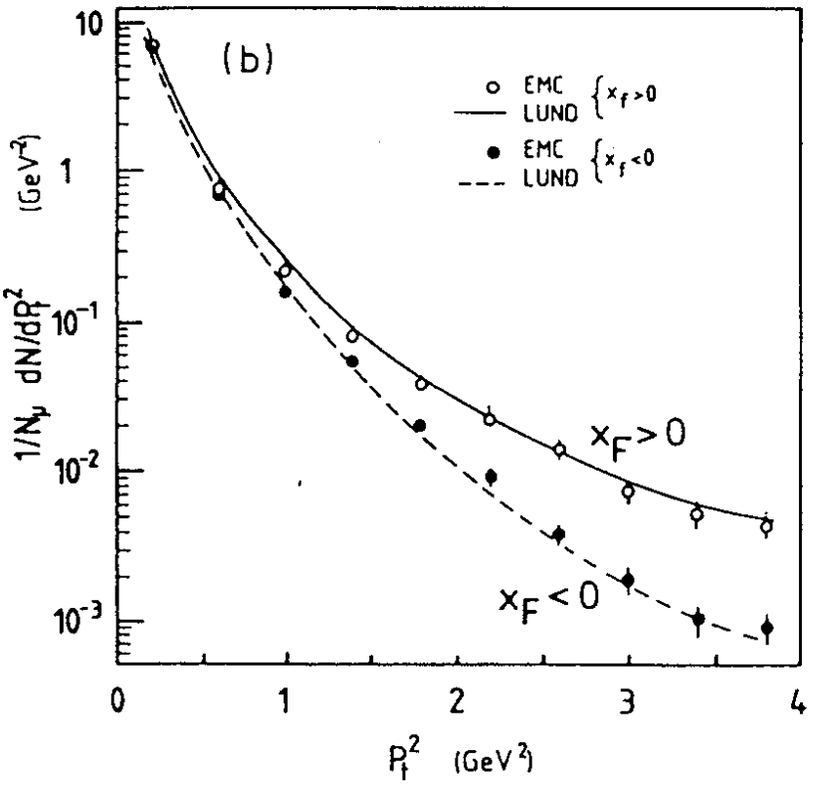
(b)
EMC
LUND
$x_f > 0$
EMC
LUND
$x_f < 0$
$x_F > 0$
$x_F < 0$
$1/N_\mu \; dN/dP_f^2$ (GeV^{-2})
P_f^2 (GeV^2)

Fig. 2

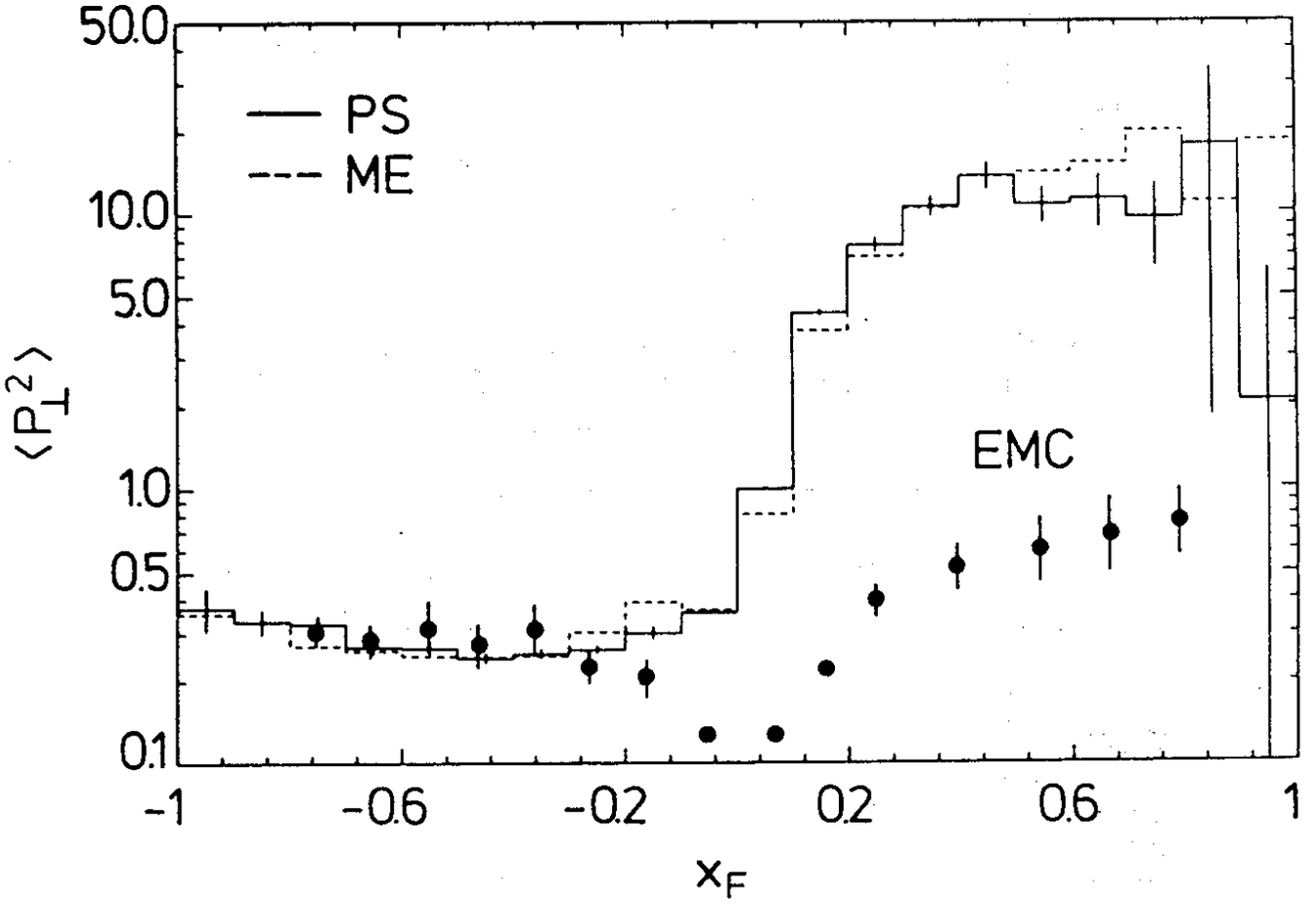
50.0
10.0
5.0
1.0
0.5
0.1
PS
ME
EMC
$\langle P_\perp^2 \rangle$
-1
-0.6
-0.2
0.2
0.6
1
x_F

Fig. 3

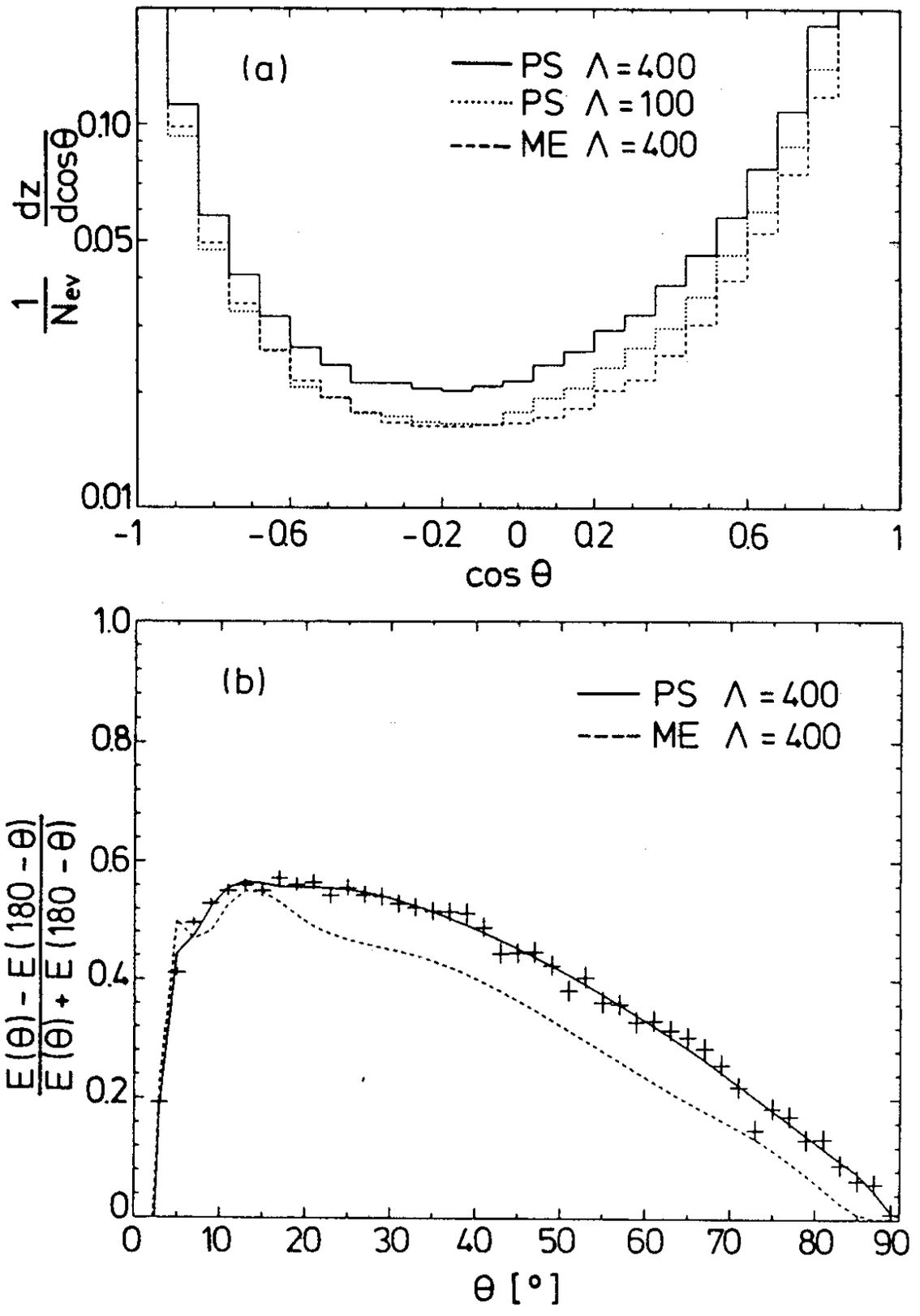
(a)
PS Λ = 400
PS Λ = 100
ME Λ = 400
1/N_ev dz/dcosθ
0.10
0.05
0.01
-1
-0.6
-0.2
0
0.2
0.6
1
cos θ
(b)
PS Λ = 400
ME Λ = 400
E(θ) - E(180 - θ) / E(θ) + E(180 - θ)
1.0
0.8
0.6
0.4
0.2
0
0
10
20
30
40
50
60
70
80
90
θ [°]

Fig. 4

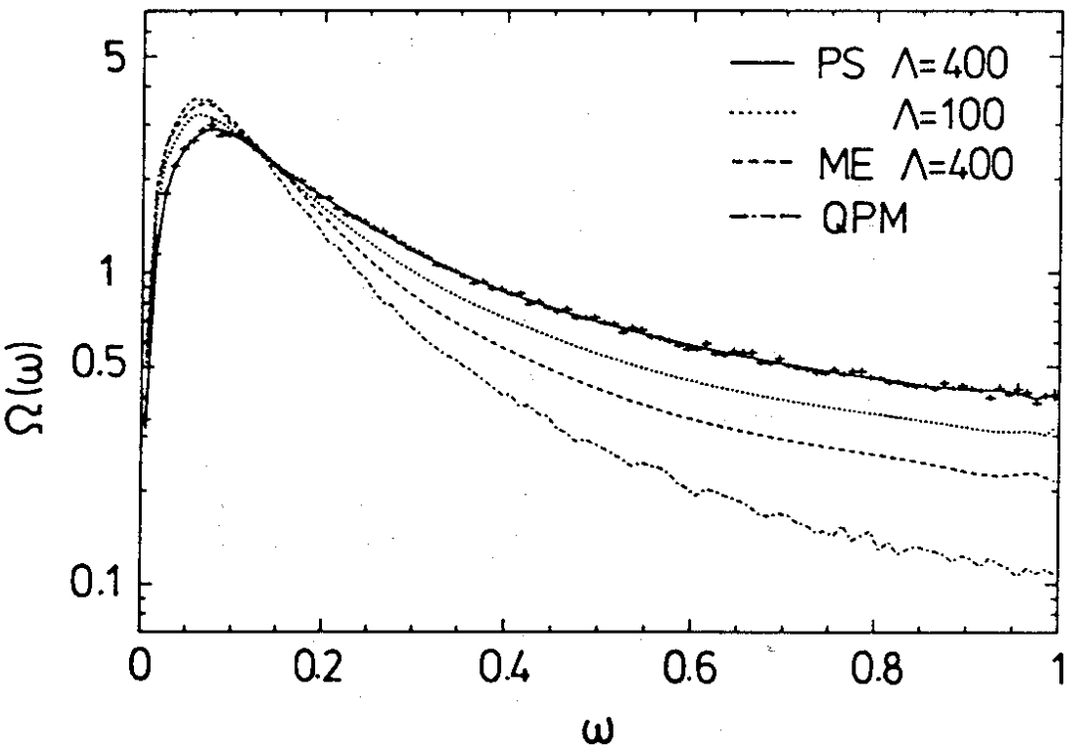
PS Λ=400
Λ=100
ME Λ=400
QPM
Ω(ω)
ω
5
1
0.5
0.1
0
0.2
0.4
0.6
0.8
1

Fig. 5

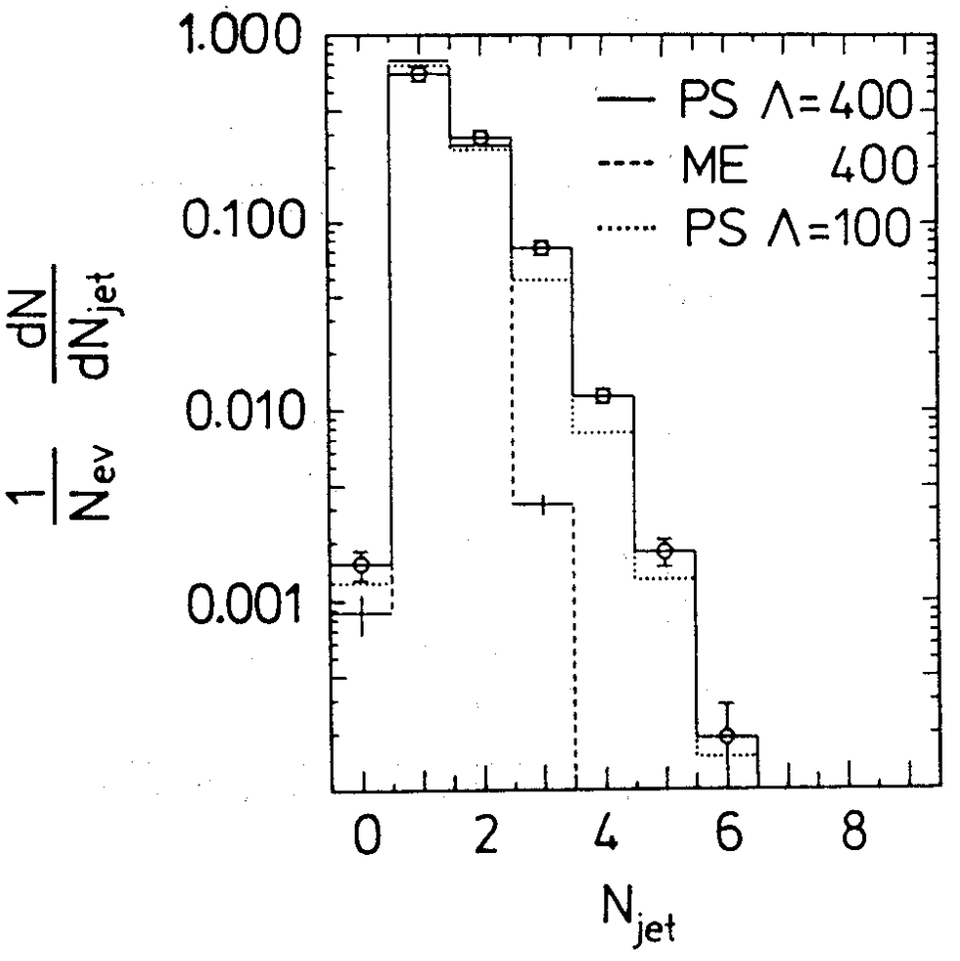
PS Λ=400
ME 400
PS Λ=100
1/N_ev dN/dN_jet
N_jet
1.000
0.100
0.010
0.001
0
2
4
6
8

Fig. 6

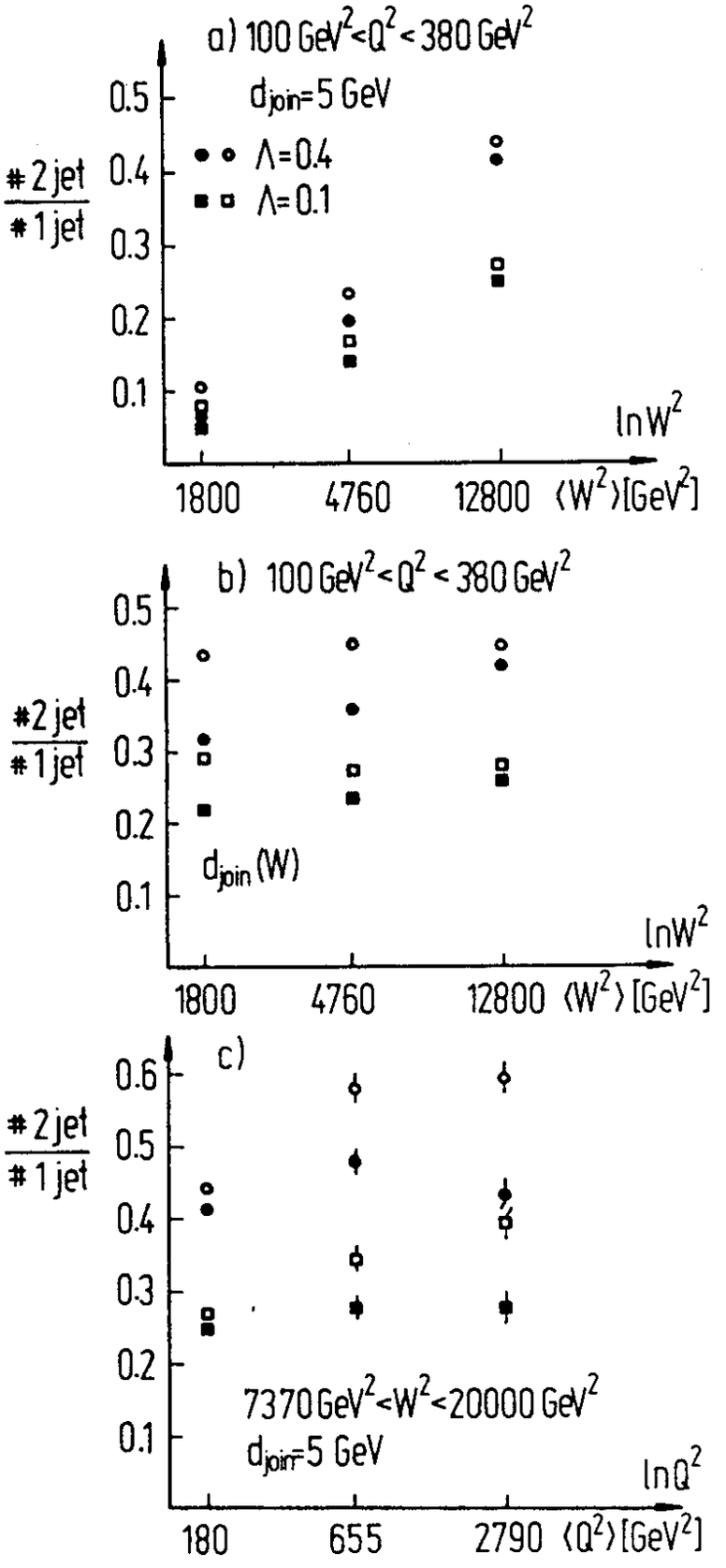
a) 100 GeV²<Q²<380 GeV²
d_join=5 GeV
Λ=0.4
Λ=0.1
#2 jet / #1 jet
0.5
0.4
0.3
0.2
0.1
ln W²
1800
4760
12800
⟨W²⟩[GeV²]
b) 100 GeV²<Q²<380 GeV²
#2 jet / #1 jet
d_join (W)
ln W²
1800
4760
12800
⟨W²⟩ [GeV²]
c)
#2 jet / #1 jet
0.6
0.5
0.4
0.3
0.2
0.1
7370 GeV²<W²<20000 GeV²
d_join=5 GeV
ln Q²
180
655
2790
⟨Q²⟩[GeV²]

Fig. 7

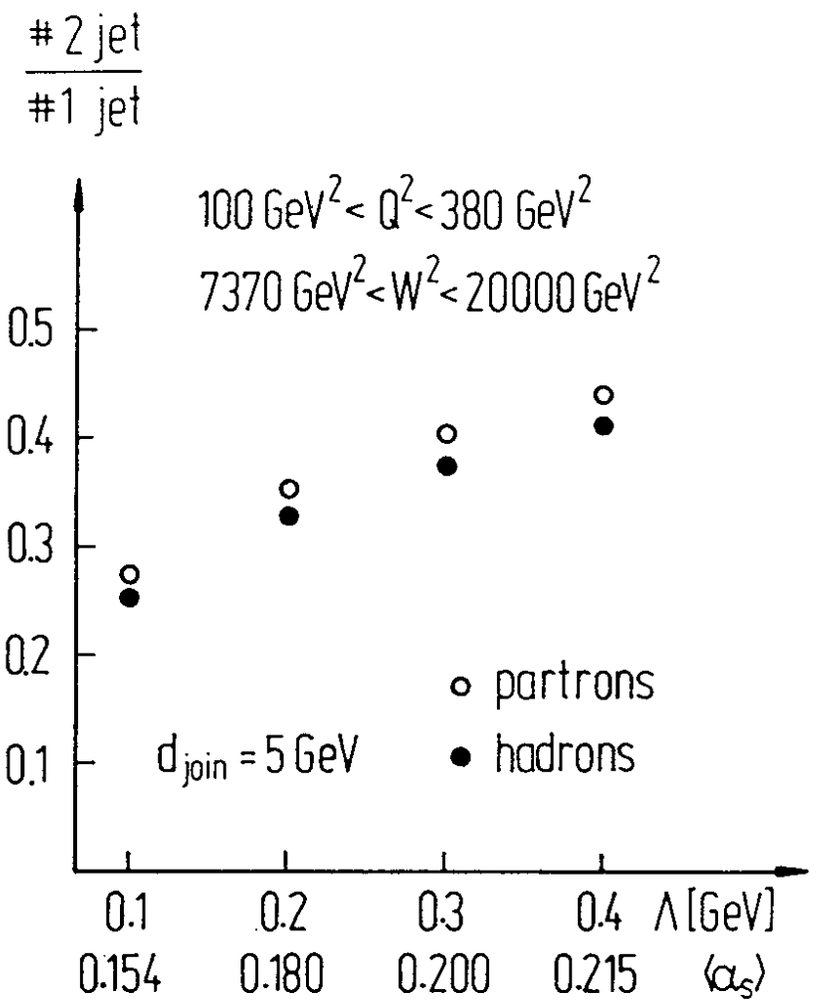
#2 jet
#1 jet
100 GeV² < Q² < 380 GeV²
7370 GeV² < W² < 20000 GeV²
0.5
0.4
0.3
0.2
0.1
partrons
hadrons
d join = 5 GeV
0.1
0.2
0.3
0.4
Λ [GeV]
0.154
0.180
0.200
0.215
⟨αs⟩

Fig. 8

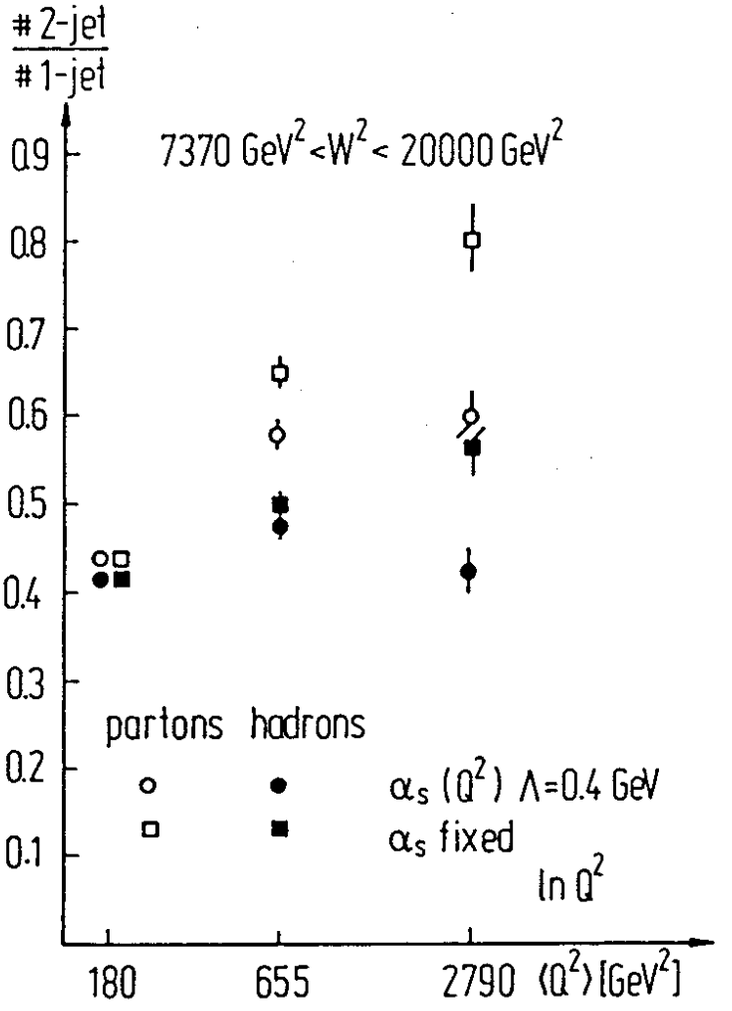
#2-jet
#1-jet
7370 GeV² < W² < 20000 GeV²
0.9
0.8
0.7
0.6
0.5
0.4
0.3
0.2
0.1
partons
hadrons
αs (Q²) Λ=0.4 GeV
αs fixed
ln Q²
180
655
2790
⟨Q²⟩ [GeV²]

Fig. 9